
Brain Perfusion Imaging Under Acetazolamide Challenge for Detection of Impaired Cerebrovascular Reserve Capacity: Positive Findings with ^{15}O -Water PET in Patients with Negative $^{99\text{m}}\text{Tc}$ -HMPAO SPECT Findings

Güliz Acker¹⁻³, Catharina Lange⁴, Imke Schatka⁴, Andreas Pfeifer⁴, Marcus A. Czabanka^{1,2}, Peter Vajkoczy^{1,2}, and Ralph Buchert⁴

¹Department of Neurosurgery, Charité-Universitätsmedizin, Berlin, Germany; ²Center for Stroke Research, Berlin, Germany; ³Berlin Institute of Health, Berlin, Germany; and ⁴Department of Nuclear Medicine, Charité-Universitätsmedizin, Berlin, Germany

Cerebrovascular reserve capacity (CVRC) is an important parameter for treatment decisions in chronic cerebrovascular diseases. It can be assessed by measuring the acetazolamide-induced change in regional cerebral blood flow using SPECT with $^{99\text{m}}\text{Tc}$ -labeled hexamethylpropyleneamine oxime ($^{99\text{m}}\text{Tc}$ -HMPAO) or PET with ^{15}O -water. **Methods:** Our database was searched for patients with moyamoya vasculopathy or atherosclerotic cerebrovascular disease who had undergone ^{15}O -water PET after normal $^{99\text{m}}\text{Tc}$ -HMPAO SPECT results with respect to CVRC. ^{15}O -water PET was analyzed visually and quantitatively. Quantitative analysis was based on parametric CVRC maps generated by voxelwise image subtraction. **Results:** The search identified 18 patients (43 ± 15 y, 12 moyamoya vasculopathy). PET revealed impaired CVRC in 8 patients (44%). Quantitative analysis confirmed the positive visual findings in ^{15}O -water PET and the negative findings in $^{99\text{m}}\text{Tc}$ -HMPAO SPECT. **Conclusion:** ^{15}O -water PET enables detection of impaired CVRC in a considerable fraction of symptomatic patients with stenocclusion and negative $^{99\text{m}}\text{Tc}$ -HMPAO SPECT.

Key Words: cerebral flow reserve; ^{15}O -water; $^{99\text{m}}\text{Tc}$ -HMPAO

J Nucl Med 2018; 59:294–298

DOI: 10.2967/jnumed.117.195818

Cerebrovascular reserve capacity (CVRC) is an important parameter in decision making for treatment of chronic stenocclusive cerebrovascular diseases such as moyamoya vasculopathy (MMV) or atherosclerotic cerebrovascular disease (ACVD). It can be assessed by imaging regional cerebral blood flow (rCBF) under pharmacologic challenge with acetazolamide compared with resting conditions. Current guidelines for the diagnosis and treatment of MMV equally recommend $^{99\text{m}}\text{Tc}$ -labeled hexamethylpropyleneamine oxime ($^{99\text{m}}\text{Tc}$ -HMPAO) SPECT and ^{15}O -water PET for this purpose (1). However, head-to-head comparison of ^{15}O -water PET and $^{99\text{m}}\text{Tc}$ -HMPAO SPECT with respect to

presurgical CVRC assessment in the same patients has not been reported so far.

Here we report the findings of ^{15}O -water PET with acetazolamide challenge in 18 patients in whom perfusion SPECT with acetazolamide challenge had been interpreted as “no evidence of impaired CVRC” and this negative SPECT finding had been suspected to be false-negative by the referring neurosurgeon.

MATERIALS AND METHODS

Eligibility Criteria

Our database was searched according to the following criteria: SPECT with $^{99\text{m}}\text{Tc}$ -HMPAO under acetazolamide challenge had been performed to assess CVRC for presurgical evaluation of symptomatic MMV or ACVD, the SPECT findings had been interpreted as “no evidence of impaired CVRC,” the negative SPECT findings had been suspected to be false-negative by the referring neurosurgeon on the basis of the patient’s symptoms, and assessment of CVRC had been repeated using ^{15}O -water PET within 4 wk.

This retrospective study was approved by the Ethics Committee of Charité-Universitätsmedizin Berlin (reference number EA4/142/16), and the requirement to obtain informed consent was waived.

$^{99\text{m}}\text{Tc}$ -HMPAO SPECT

Resting brain perfusion SPECT was performed 40 min after intravenous administration of 510.3 ± 62.2 MBq of $^{99\text{m}}\text{Tc}$ -HMPAO. On the next day or the day afterward, perfusion SPECT was repeated 5–15 min after infusion (2.5 mL/min) of 1,000 mg of acetazolamide in 50 mL of 0.9% NaCl (513.3 ± 62.4 MBq; paired *t* test, *P* = 0.708). A GE Healthcare Millennium VG Hawkeye or a Siemens MultiSPECT 3 camera was used for SPECT (same camera for resting and acetazolamide scan in each patient). Images were reconstructed using filtered backprojection with the same Butterworth filter in all cases (cutoff, 0.5 cycles/cm; 10th order; Chang attenuation correction with $\mu = 0.12$ cm⁻¹; no scatter correction). Spatial resolution in the reconstructed SPECT images was about 13 mm in full width at half maximum.

^{15}O -Water PET

Brain perfusion PET was performed with 700 MBq of ^{15}O -water and a Philips Gemini TF16 PET/CT system. The time of arrival of ^{15}O -water in the brain was determined from the whole-brain time-activity curve. A static ^{15}O -water uptake image was obtained by iterative reconstruction of 40 s of list-mode data starting at this time point (3-dimensional line-of-response algorithm of the system software with

Received May 6, 2017; revision accepted Jun. 27, 2017.

For correspondence or reprints contact: Ralph Buchert, Department of Nuclear Medicine, University Medical Center Hamburg-Eppendorf, 20246 Hamburg, Germany.

E-mail: r.buchert@uke.de

Published online Jul. 20, 2017.

COPYRIGHT © 2018 by the Society of Nuclear Medicine and Molecular Imaging.

default parameter settings, CT-based attenuation correction). Infusion of acetazolamide was initiated immediately after the resting perfusion PET scan using the same dose and infusion protocol as for the SPECT scan. ^{15}O -water PET was repeated 5–15 min after acetazolamide infusion. Spatial resolution in the reconstructed PET images was about 7 mm in full width at half maximum.

Parametric Maps of Relative CVRC (rCVRC)

rCVRC was estimated voxelwise to generate a 3-dimensional rCVRC map (Fig. 1). This was done separately for SPECT and PET using an automated processing pipeline comprising the following steps. First, the SPECT or PET image is smoothed with an isotropic 3-dimensional gaussian kernel of 8 mm (SPECT) or 6 mm (PET) in full width at half maximum. Second, the Statistical Parametric Mapping (SPM8) “coregister” tool (Wellcome Trust Centre for Neuroimaging) is used to estimate the rigid-body transformation that maps the acetazolamide image to the resting image. Third, the SPM8 “normalize” tool is used to map the resting and the coregistered acetazolamide image into SPM’s template space. Fourth, images are smoothed with an isotropic gaussian kernel of 20 mm in full width at half maximum. Finally, the rCVRC map is computed voxel by voxel as

$$\text{rCVRC (\%)} = 100 \times (\text{sf} \times \text{swA} - \text{swR}) / \text{swR}, \quad \text{Eq. 1}$$

where swA and swR denote the smoothed, anatomically standardized uptake image under acetazolamide or resting conditions, respectively. The computation of rCVRC is restricted to a binary cerebrum mask that was obtained by thresholding the SPM8 gray matter probability map at 0.3.

The scale factor sf in Equation 1 accounts for (small) variations in the administered tracer dose between resting and acetazolamide conditions. It is determined such that the average rCVRC over a reference region (defined below) is 30% (2), that is,

$$\text{sf} = 1.3 / \text{mean}_{\text{Ref}}(\text{swA}/\text{swR}), \quad \text{Eq. 2}$$

where mean_{Ref} is the mean value over the reference region. The reference region is intended to include all “normal” voxels within the cerebrum mask, that is, voxels with normal perfusion both in the resting and in the acetazolamide scans. Normal voxels were determined independently for resting and acetazolamide scans using the following iterative 2-step approach and starting with all voxels in the cerebrum mask. First, all voxels with an intensity below the fifth percentile were removed. Second, the mean intensity of the remaining voxels was compared with the mean intensity of the normal voxels in the preceding iteration. The 2 steps were repeated until the mean intensity of normal voxels changed less than 1%. The iterative procedure worked properly according to visual inspection in all cases (contour delineating normal voxels overlaid to transversal images). The reference region was obtained as the intersection of normal voxels from the resting scan and normal voxels from the acetazolamide scan.

Visual Interpretation

Visual interpretation of SPECT and PET was supported by a PDF document (created by the automatic processing pipeline) with standardized side-by-side display of anatomically normalized resting and acetazolamide images together with the rCVRC map (Fig. 1). Visual interpretation with respect to presence or absence of CVRC impairment was performed independently by 2 experienced readers masked to clinical information.

Quantitative Analysis of CVRC

Defects

CVRC defects were defined by thresholding the rCVRC map at 15% (i.e., 50% reduction from the normal rCVRC of 30%). The volume of the CVRC defect and the mean rCVRC within the defect were computed.

RESULTS

Patients

Eligibility criteria were fulfilled by 18 of 155 patients who had undergone $^{99\text{m}}\text{Tc}$ -HMPAO SPECT for presurgical evaluation of symptomatic MMV or ACVD between January 2012 and October 2015 at our institution (12%). Demographics and clinical data are given in Table 1. The time interval between PET and SPECT was less than 1 wk in all but 2 patients (8 and 27 d). None of the patients had a cerebrovascular event between SPECT and PET.

CVRC

Visual interpretation confirmed “no evidence of impaired CVRC” in $^{99\text{m}}\text{Tc}$ -HMPAO SPECT in any cases. Visual interpretation of ^{15}O -water PET revealed CVRC reduction in 8 patients (44%) (Fig. 2).

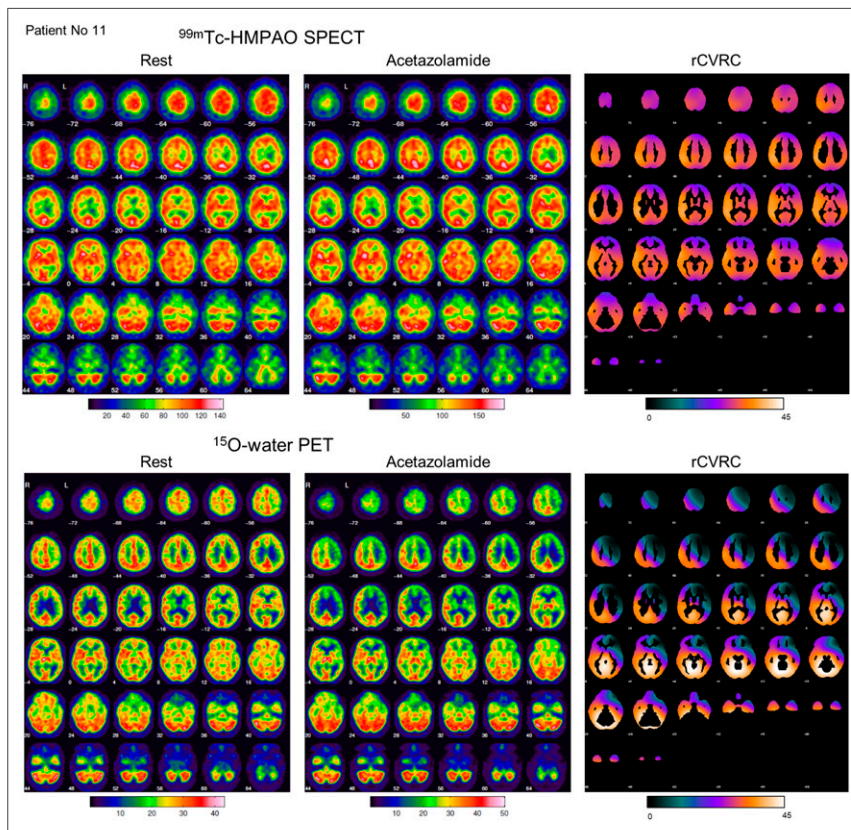


FIGURE 1. Standardized display to support visual interpretation of $^{99\text{m}}\text{Tc}$ -HMPAO SPECT (top) and ^{15}O -water PET (bottom) with respect to impairment of rCVRC.

TABLE 1
Patient Characteristics

Patient no.	Sex	Age (y)	Disease	Stenoocclusion	Infarction	Symptoms	Symptomatic hemisphere	Impaired CVRC on PET
1	F	19	MMV	Bi	BZ L	Ischemic event	L	None
2	M	20	MMV	Bi	Territorial R, BZ L	Ischemic event+hemorrhage	L	None
3	F	24	MMV	Bi	BZ Bi	Ischemic event	R	None
4	F	26	MMV	Bi	BZ Bi	Ischemic event	R	None
5	M	27	Uni MMV	Uni	None	Ischemic event	R	None
6	F	28	Uni MMV	Uni	BZ L	Headache	Both	None
7	F	45	Uni MMV	Bi	BZ R	Ischemic event	R	None
8	F	46	MMV	Bi	BZ Bi	Ischemic event	R	Bi
9	F	47	MMV	Bi	BZ Bi	Ischemic event	R	R
10	M	47	ACVD	Uni	BZ R	Ocular ischemic syndrome	R	None
11	F	49	MMV	Bi	BZ R	Ischemic event	L	L
12	F	49	Quasi MMV	Bi	None	Ischemic event+hemorrhage	L	L
13	M	54	ACVD	Bi	BZ Bi	Ischemic event	L	Bi
14	F	54	Uni MMV	Uni	None	Ischemic event+hemorrhage	L	L
15	M	57	ACVD	Bi	BZ Bi, lacunar R	Ischemic event	R	None
16	M	59	ACVD	Uni	BZ L	Ischemic event	L	L
17	M	60	ACVD	Bi	Lacunar R	Ocular ischemic syndrome+syncope	R	None
18	F	67	ACVD	Uni	BZ R	Ischemic event	R	R

Bi = bilateral; Uni = unilateral; BZ = border zone.

Hemisphere-based evaluation of ^{15}O -water PET showed CVRC reduction in 10 of 30 hemispheres with stenoocclusion. All the patients and 80% of the hemispheres with reduced CVRC were primary symptomatic, suggesting the PET finding to be true-positive (Table 1).

The volume of the CVRC lesions ranged from 79 to 696 mL (Table 2; Fig. 2), with a mean rCVRC in the defect ranging from -2.1% to 12.7%.

Visual evaluation of the resting ^{15}O -water PET images of the 8 patients with CVRC reduction (first column in Fig. 2) revealed normal resting rCBF in the CVRC defect (i.e., stage I impairment of cerebral hemodynamics according to Powers' classification (3), so-called autoregulatory vasodilatation) in 3 of the 8 patients (37.5%), mildly reduced resting rCBF (early stage II impairment, autoregulatory failure) in 4 patients (50%), and moderately reduced resting rCBF (advanced stage II) in one patient (12.5%).

For quantitative comparison of SPECT and PET CVRC, the outer contour of the defect (delineated in the PET rCVRC map) was copied to the SPECT rCVRC map (Fig. 2). SPECT rCVRC in PET lesions ranged from 23.9% to 34.6% (Table 2). SPECT rCVRC was significantly larger than PET rCVRC ($P < 0.0005$). SPECT rCVRC in the PET rCVRC lesions was not significantly different from the normal value of 30% ($P = 0.802$).

DISCUSSION

The main finding of the present study was that brain PET with ^{15}O -water enables detection of impaired CVRC in a considerable fraction of symptomatic MMV and ACVD patients in whom $^{99\text{m}}\text{Tc}$ -HMPAO SPECT is negative, that is, does not show impairment of CVRC.

PET provides better spatial resolution and better count sensitivity than SPECT, the latter allowing for better statistical image quality in PET after administration of standard tracer doses. Mislocalization of scattered photons also contributes to the underestimation of rCBF contrast between high and low rCBF in SPECT (without scatter correction) compared with PET (with scatter correction). Furthermore, the kinetics of ^{15}O -water (freely diffusible and inert) makes ^{15}O -water PET a better marker of rCBF than $^{99\text{m}}\text{Tc}$ -HMPAO SPECT (4,5). $^{99\text{m}}\text{Tc}$ -HMPAO is based on the principle of "chemical microspheres," according to which the tracer is fully extracted from arterial blood to tissue during a single capillary passage and then is locally retained in the tissue. In case of $^{99\text{m}}\text{Tc}$ -HMPAO, fixation in tissue is due to glutathione-dependent metabolism to hydrophilic forms and binding to nondiffusible cell components (6,7). However, the kinetics of $^{99\text{m}}\text{Tc}$ -HMPAO shows considerable violation of the microsphere principle. First, glutathione-dependent metabolism is not fast enough

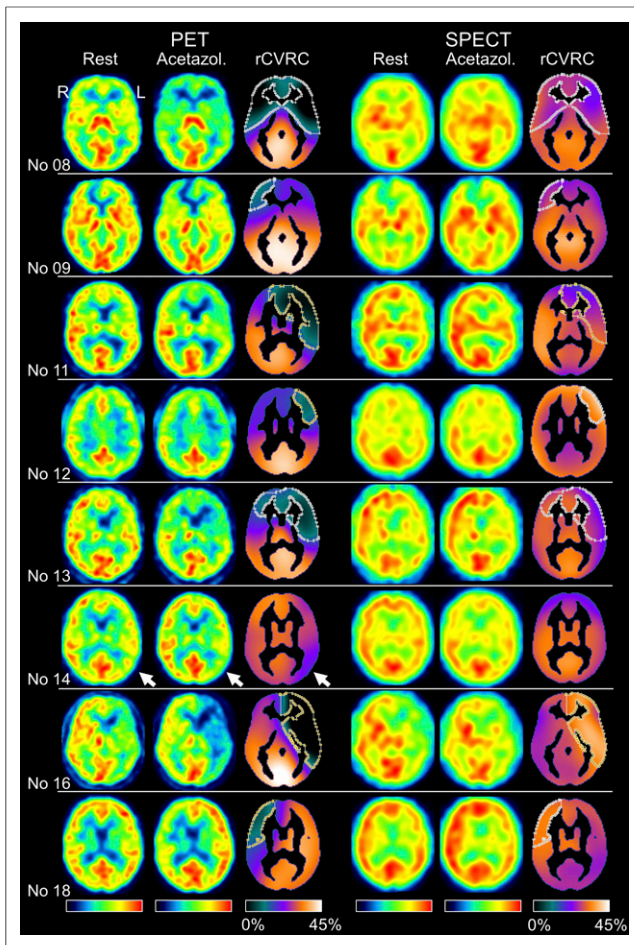


FIGURE 2. Patients with impaired CVRC according to visual interpretation of ^{15}O -water PET despite “no evidence of impaired CVRC” in the $^{99\text{m}}\text{Tc}$ -HMPAO SPECT images. Columns 1 to 3 show representative transversal slice of ^{15}O -water PET at rest and under acetazolamide challenge together with rCVRC map. Contour in rCVRC map delineates CVRC defect obtained by thresholding rCVRC map at 15% (i.e., 50% reduction from normal rCVRC set to 30%). CVRC reduction in left temporooccipital cortex in patient 14 (arrows) did not reach this threshold. Columns 4 to 6 show same slice in $^{99\text{m}}\text{Tc}$ -HMPAO SPECT images. Contour in SPECT CVRC map is copy of contour from PET CVRC map.

to avoid clearance of unmetabolized $^{99\text{m}}\text{Tc}$ -HMPAO from tissue (8). Second, in resting conditions, only about 70% of $^{99\text{m}}\text{Tc}$ -HMPAO in blood is extracted to tissue during a single capillary passage (9). The extraction fraction further decreases with increasing rCBF. As a consequence, the acetazolamide-induced increase of local $^{99\text{m}}\text{Tc}$ -HMPAO uptake underestimates the actual increase of rCBF. The fraction of unmetabolized $^{99\text{m}}\text{Tc}$ -HMPAO cleared from tissue before fixation will also increase with increasing rCBF (9). This adds to the deficit by which the percentage increase of $^{99\text{m}}\text{Tc}$ -HMPAO retained in tissue lags behind the acetazolamide-induced increase of rCBF. These limiting effects are smaller for ^{15}O -water because of its generally higher extraction fraction (10). This, together with improved image quality of PET compared with SPECT, most likely results in improved sensitivity for the detection of impaired CVRC by acetazolamide challenge, which would explain the findings of this study.

A major limitation of the study is its restriction to patients with negative $^{99\text{m}}\text{Tc}$ -HMPAO SPECT results, which prevents

estimation of diagnostic performance in terms of sensitivity, specificity, and predictive values. It particularly eliminates the potential to discover cases in which ^{15}O -water PET is negative and $^{99\text{m}}\text{Tc}$ -HMPAO SPECT is positive.

The strength of the present study is that it is the first head-to-head comparison of $^{99\text{m}}\text{Tc}$ -HMPAO SPECT and ^{15}O -water PET for assessment of CVRC in patients with cerebral stenocclusive diseases. Kuwabara et al. compared $^{99\text{m}}\text{Tc}$ -HMPAO SPECT and ^{15}O -water PET in patients with cerebral infarction and crossed cerebellar diaschisis (CCD) with respect to acetazolamide response in the cerebellum (CVRC in the cerebrum, the measure of interest in presurgical evaluation of MMV or ACVD patients, was not assessed in this study) (11). The acetazolamide-induced increase of cerebellar blood flow as measured by ^{15}O -water PET did not differ between the CCD and the non-CCD side, whereas the percentage increase of cerebellar counts in $^{99\text{m}}\text{Tc}$ -HMPAO SPECT was significantly smaller in the non-CCD side (11). This obscuring of CCD after acetazolamide challenge in $^{99\text{m}}\text{Tc}$ -HMPAO SPECT most likely was caused by more pronounced underestimation of acetazolamide-induced rCBF increase in the non-CCD side of the cerebellum because of its higher resting rCBF, in line with the present study.

Matsumoto et al. evaluated SPECT with $^{99\text{m}}\text{Tc}$ -labeled ethyl cysteinate dimer ($^{99\text{m}}\text{Tc}$ -ECD) for detection of misery perfusion in patients with unilateral chronic occlusive disease (12). Increased oxygen extraction fraction as measured by PET with ^{15}O gas was used as the gold standard. The area under the receiver-operating-characteristic curve for detection of misery perfusion by the ipsilateral-to-contralateral $^{99\text{m}}\text{Tc}$ -ECD uptake in the supply territory of the middle cerebral artery increased from 0.780 to 0.974 ($P = 0.0001$) when the $^{99\text{m}}\text{Tc}$ -ECD uptake ratio in the middle cerebral artery territory was scaled to the contralateral-to-ipsilateral ratio of $^{99\text{m}}\text{Tc}$ -ECD uptake in the cerebellum (12). This was due to crossed cerebellar hypoperfusion (12). These findings suggest that the accuracy of brain perfusion SPECT with chemical microspheres such as $^{99\text{m}}\text{Tc}$ -ECD and $^{99\text{m}}\text{Tc}$ -HMPAO for detection of hemodynamic impairment can be considerably improved

TABLE 2
Quantitative Characterization of CVRC Defects in Patients with Impaired CVRC According to Visual Inspection of ^{15}O -Water PET

Patient no.	Defect volume (mL)	Mean CVRC PET (%)	Mean CVRC SPECT (%)
8	696	6.1	28.1
9	79	12.7	23.9
11	437	7.2	26.5
12	137	11.8	34.6
13	426	10.9	26.9
14	0		
16	517	-2.1	34.4
18	168	10.8	32.7

CVRC reduction in left temporooccipital cortex in patient 14 did not reach threshold for automatic delineation (Fig. 2).

by combining supratentorial tracer uptake with cerebellar tracer uptake, at least in patients with unilateral chronic occlusive disease.

CONCLUSION

^{15}O -water brain PET under acetazolamide challenge enables detection of impaired CVRC in a considerable fraction of symptomatic patients with stenooclusive cerebral disease and negative $^{99\text{m}}\text{Tc}$ -HMPAO SPECT results. ^{15}O -water PET is limited in availability to facilities with an on-site cyclotron and radiochemistry support. Symptomatic patients with stenooclusive cerebral disease and $^{99\text{m}}\text{Tc}$ -HMPAO SPECT suspected to be false negative (~10% of all patients) might be referred to a specialized PET center for ^{15}O -water PET.

DISCLOSURE

Dr. Acker is a participant of the BIH-Charité Clinician Scientist Program funded by the Charité-Universitätsmedizin Berlin and the Berlin Institute of Health. No other potential conflict of interest relevant to this article was reported.

REFERENCES

1. Research Committee on the Pathology and Treatment of Spontaneous Occlusion of the Circle of Willis; Health Labour Sciences Research Grant for Research on Measures for Intractable Diseases. Guidelines for diagnosis and treatment of moyamoya disease (spontaneous occlusion of the circle of Willis). *Neurol Med Chir (Tokyo)*. 2012;52:245–266.
2. Okazawa H, Yamauchi H, Sugimoto K, Toyoda H, Kishibe Y, Takahashi M. Effects of acetazolamide on cerebral blood flow, blood volume, and oxygen metabolism: a positron emission tomography study with healthy volunteers. *J Cereb Blood Flow Metab*. 2001;21:1472–1479.
3. Powers WJ. Cerebral hemodynamics in ischemic cerebrovascular disease. *Ann Neurol*. 1991;29:231–240.
4. Raichle ME, Martin WR, Herscovitch P, Mintun MA, Markham J. Brain blood flow measured with intravenous H_2^{15}O . II. Implementation and validation. *J Nucl Med*. 1983;24:790–798.
5. Kuwabara Y, Ichiya Y, Otsuka M, et al. Comparison of I-123 IMP and Tc-99m HMPAO SPECT studies with PET in dementia. *Ann Nucl Med*. 1990;4:75–82.
6. Colamussi P, Calo G, Sbrenna S, et al. New insights on flow-independent mechanisms of $^{99\text{m}}\text{Tc}$ -HMPAO retention in nervous tissue: in vitro study. *J Nucl Med*. 1999;40:1556–1562.
7. Neirinckx RD, Burke JF, Harrison RC, Forster AM, Andersen AR, Lassen NA. The retention mechanism of technetium-99m-HM-PAO: intracellular reaction with glutathione. *J Cereb Blood Flow Metab*. 1988;8(suppl):S4–S12.
8. Lassen NA, Andersen AR, Friberg L, Paulson OB. The retention of [$^{99\text{m}}\text{Tc}$]-d,l-HM-PAO in the human brain after intracarotid bolus injection: a kinetic analysis. *J Cereb Blood Flow Metab*. 1988;8(suppl):S13–S22.
9. Andersen AR, Friberg HH, Schmidt JF, Hasselbalch SG. Quantitative measurements of cerebral blood flow using SPECT and [$^{99\text{m}}\text{Tc}$]-d,l-HM-PAO compared to xenon-133. *J Cereb Blood Flow Metab*. 1988;8(suppl):S69–S81.
10. Go KG, Lammertsma AA, Paans AM, Vaalburg W, Woldring MG. Extraction of water labeled with oxygen 15 during single-capillary transit: influence of blood pressure, osmolarity, and blood-brain barrier damage. *Arch Neurol*. 1981;38:581–584.
11. Kuwabara Y, Ichiya Y, Sasaki M, et al. Cerebellar vascular response to acetazolamide in crossed cerebellar diaschisis: a comparison of $^{99\text{m}}\text{Tc}$ -HMPAO single-photon emission tomography with ^{15}O -H $_2\text{O}$ positron emission tomography. *Eur J Nucl Med*. 1996;23:683–689.
12. Matsumoto Y, Oikawa K, Nomura JI, et al. Optimal brain $^{99\text{m}}\text{Tc}$ -ethyl cysteinyl dimer SPECT imaging and analysis to detect misery perfusion on ^{15}O PET imaging in patients with chronic occlusive disease of unilateral major cerebral artery. *Clin Nucl Med*. 2017;42:499–505.